

# Flexible Tactile Sensors Using Screen-Printed P(VDF-TrFE) and MWCNT/PDMS Composites

Saleem Khan, Sajina Tinku, Leandro Lorenzelli, *Member, IEEE*, and Ravinder S. Dahiya, *Senior Member, IEEE*

**Abstract**—This paper presents and compares two different types of screen-printed flexible and conformable pressure sensors arrays. In both variants, the flexible pressure sensors are in the form of segmental arrays of parallel plate structure—sandwiching the piezoelectric polymer polyvinylidene fluoride trifluoroethylene [P(VDF-TrFE)] between two printed metal layers of silver (Ag) in one case and the piezoresistive [multiwall carbon nanotube (MWCNT) mixed with poly(dimethylsiloxane (PDMS))] layer in the other. Each sensor module consists of  $4 \times 4$  sensors array with  $1\text{-mm} \times 1\text{-mm}$  sensitive area of each sensor. The screen-printed piezoelectric sensors array exploits the change in polarization level of P(VDF-TrFE) to detect dynamic tactile parameter such as contact force. Similarly, the piezoresistive sensors array exploits the change in resistance of the bulk printed layer of MWCNT/PDMS composite. The two variants are compared on the basis of fabrication by printing on plastic substrate, ease of processing and handling of the materials, compatibility of the dissimilar materials in multilayers structure, adhesion, and finally according to the response to the normal compressive forces. The foldable pressure sensors arrays are completely realized using screen-printing technology and are targeted toward realizing low-cost electronic skin.

**Index Terms**—Screen printing, flexible electronics, tactile sensors, piezoelectric sensors, piezoresistive sensors.

## I. INTRODUCTION

PRINTED electronics and sensors over large areas and diverse substrates is growing rapidly due to attractive features such as low-cost processing and possibility of depositing diverse materials over nonplanar surfaces. The rapid growth of the field is in line with the electronics roadmap, which indicates the merge of the well-established microelectronics technology with the age-old printing tools to realize electronic systems with simplified processing steps, reduced materials wastage, high throughput, low fabrication cost and single patterned deposition processes [1], [2].

Manuscript received June 16, 2014; revised October 21, 2014; accepted October 31, 2014. Date of publication November 26, 2014; date of current version April 16, 2015. This work was supported in part by the European Commission under Grant Agreements PITN-GA-2012-317488-CONTEST, EPSRC Fellowship for Growth – PRINTSKIN (EP/M002527/1) and EPSRC First Grant - FLEXELDEMO (EP/M002519/1). The associate editor coordinating the review of this paper and approving it for publication was Prof. Madhusudan Singh.

S. Khan, S. Tinku, and L. Lorenzelli are with the University of Trento, Trento 38100, Italy, and also with the Microsystems Technology Research Unit, Fondazione Bruno Kessler, Trento 38122, Italy (e-mail: skhan@fbk.eu; tinku@fbk.eu; lorenzel@fbk.eu).

R. S. Dahiya is with the Department of Electronics and Nanoscale Engineering, School of Engineering, University of Glasgow, Glasgow G12 8QQ, U.K. (e-mail: ravinder.dahiya@glasgow.ac.uk).

Color versions of one or more of the figures in this paper are available online at <http://ieeexplore.ieee.org>.

Digital Object Identifier 10.1109/JSEN.2014.2368989

Amongst various active and passive flexible electronic devices developed so far, the research on electronic or tactile skin for robotics has gained significant interest due to the future needs in applications such as prosthetic devices, safe human-robot interaction and multitasks for handling delicate structures [3]. As robot technology advances, the significance of tactile sensors increases as it enables robots to conduct practical tasks such as grasping and handling delicate objects [3]–[7]. Tactile sensors over large areas such as entire body of a humanoid robot or of an industrial manipulator will open new research area in robotic whereby whole body contacts could be exploited to carry out such as lifting a large box or lifting an elderly – as humans do. The ultra-flexible and lightweight electronic or tactile skin with capability to measure the contact parameters such as pressure, temperature and proximity or soft-touch is the key enabler for above tasks and applications.

Typical manipulation tasks such as grasping, picking and placing an object from one place to another are divided amongst various action phases [8]. To successfully carry out such manipulation tasks humans require dynamic tactile feedback (e.g. from fast adapting receptors in the skin) at transition of action phases and static or quasi-static tactile feedback (e.g. from slow adapting receptors in the skin) during the course of an action phase. The implication of these studies in humans on robotics is that the tactile skin should comprise of sensors or transducers capable of detecting both the static and dynamic contact events [4]. This is also the motivation behind investigating both the piezoelectric and piezoresistive sensors in this work. Whereas the former detects the dynamic events, the latter is capable of measuring static or quasi-static contacts. Considering human touch sensing as reference, the tactile sensors should be able to detect dynamic contact forces up to 1 kHz.

On practical side, the cost-effectiveness of electronic or tactile skin, especially of the large area skin, plays a major role in its effective use in robotics. For this reason, the printing technologies are attractive and an all screen-printing technique is the possible alternative available [9]–[13]. The possibility of fast production of sensors over large areas makes screen-printing attractive for manufacturing. Screen printing method has been used in this paper to develop the piezoelectric and piezoresistive tactile sensors. In particular, the focus of investigations in this paper is on the manufacturing processes, number of steps involved in the final module development, ease of handling of materials, compatibility of dissimilar materials in multilayer structures, adhesion to polymer substrate,

overall assembly of the sensor modules and finally on the basis of sensor response to normal compressive forces.

This paper is organized as follows – The Section II presents briefly the state of the art relevant to this work. The state of art has been divided in two subsections – first describing the works related to piezoelectric and piezoresistive tactile sensors, and the second describing various printing technologies. The materials and solution synthesis are discussed in Section III. This is followed by screen-printing related experiments in Section IV. The results related to the printed structures are presented in Section V. Finally, conclusion, and future scope are given in section VI.

## II. STATE OF THE ART

### A. Piezoelectric and Piezoresistive Tactile Sensors

Over the years, wide varieties of tactile sensing structures have been demonstrated using various transduction methods such as capacitive, ultrasonic, piezoresistive, and piezoelectric etc. [14]–[16]. Piezoelectric materials are unique as they allow measuring dynamic events such as slippage and have wider applicability in sensors, actuators and energy harvesters [17]–[20]. Amongst various piezoelectric materials, the Polyvinylidene fluoride (PVDF) and its copolymer Trifluoroethylene (TrFE) have been widely investigated due to their mechanical flexibility and stable piezo, pyro and ferroelectric properties. Attractive features of P(VDF-TrFE) are the high sensitivity, wide frequency response, flexibility, cost effectiveness, and ease of fabrication [5], [16], [20], [21].

Piezoresistance is another interesting phenomenon that has been exploited to develop pressure sensors (e.g. for grip) for measuring static contact events. Their advantages include simple low-cost electronics [4], [22], [23]. Several materials and mechanisms explored to exploit piezoresistance for sensor include change in resistance of metallic strain gauges or change in mobility of solid-state semiconductor devices [24]–[26]. Often these materials and structures have low gauges factors and to overcome this obstacle, the conductive polymer composites have been explored by researchers to develop piezoresistive devices. MWCNT in PDMS (polydimethylsiloxane) matrix results in a material which possesses a number of exciting properties that can successfully be harnessed in sensors and actuators [27]–[33].

### B. Printing Technologies

For deployment of sensor arrays on large surfaces, it is necessary to micro-pattern the transducer material in an efficient and cost-effective way. Different fabrication technologies have been reported to realize P(VDF-TrFE) and MWCNT/PDMS based sensors. Spin coating, thermally drawn functional fibers, micro-machined mold transfer, single and multilayer inkjet printers have been employed for deposition of these solutions for sensors [6], [20], [21], [29], [30], [34]–[38]. The frequently used techniques such as spin coater and inkjet for patterning large areas devices have limitations of process speed and overlay registration accuracy in multilayered structures. Although, inkjet printing has high lateral resolution, patterning of large areas (> 2 mm) require repeated deposition of droplets,

which often results in a nonuniform layer thickness and edges. In addition, patterning of P(VDF-TrFE) after spin coating whole layer on wafer requires photolithography, which leads to more complexity of the manufacturing process [20]. The cost-effectiveness and faster fabrication of sensors over large areas make screen-printing very attractive and therefore [11], [12], an all screen-printed structure is the main focus of our current study. Using the same technology for all the layers will help in minimizing processing time and improve manufacturability. Besides this, the use of printing technologies will lead to reduce material waste and high-speed manufacturing.

## III. MATERIALS SYNTHESIS AND SCHEME OF THE SENSORS

### A. PVDF-TrFE Solution Preparation

The materials used for developing piezoelectric modules consist of P(VDF-TrFE) as the transducer medium. PVDF is a well-known polymer used in piezoelectric based sensors due to excellent features especially for dynamic responses of compressive forces, which can be successfully harnessed for tactile sensing in robotic skin for slip detection and control. Usually mechanical stretching is required to induce piezoelectric properties into PVDF, which is incompatible with microfabrication process. On the other hand, P(VDF-TrFE) has the tendency to crystallize directly in the polar  $\beta$ -phase without any requirements of mechanical stretching [4], [39]. Molecular proportion  $x$  ( $0.6 < x < 0.85$ ) of the vinylidene fluoride in P(VDF-TrFE) define the crystal structure and optimal piezoelectricity of the polymers [5], [20]. Compositions around 70/30%wt. exhibit good ferroelectric response.

P(VDF-TrFE) have good solubility in Dimethylformamide (DMF) and Methyl Ethyl Ketone (MEK) which are most appropriate for screen-printing. Solutions with different weight ratios of P(VDF-TrFE) and MEK were investigated for optimum parameters of dispensing through stencil mask of a screen-printing. Pallets of 70/30%wt. P(VDF-TrFE) were dissolved in Methyl Ethyl Ketone (MEK) at 15% weight to get the solution compatible with screen printing experiments [11]. After mechanical stirring, the mixture was kept at 90°C for 6 hours and stirred continuously. This resulted in P(VDF-TrFE) pallets were completely dissolved in MEK and solution was used with screen-printing without any further treatments.

### B. MWCNT/PDMS Nanocomposite Preparation

Development of piezoresistive sensors array consisted of multiwall carbon nanotube (MWCNT) mixed with Poly(dimethyl-siloxane) (PDMS) matrix. Incorporating the MWCNTs in PDMS results in a material with a number of exciting properties for sensors and actuators especially for grip purposes in tactile sensors of robotic skin. The actuation mechanism is based on the geometry and interconnection paths of nanotubes developed in the polymer matrix, which vary upon application of force. This leads to a change in resistance of the bulk composite layer [28], [29], [38]. These nanocomposite materials have similar characteristics to some inorganic semiconductors while maintaining typical

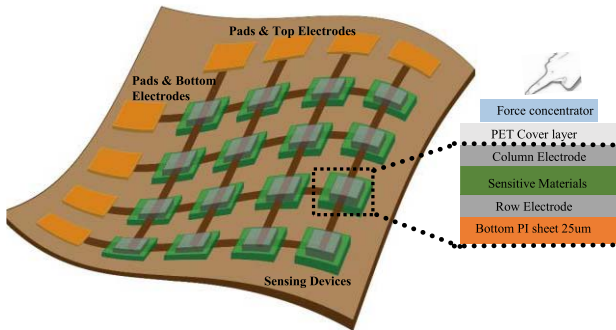


Fig. 1. Schematic diagram of a single module of sensors array and cross sectional view of the proposed printed layers.

polymer properties of flexibility, easy processing and synthesis. A low percolation threshold is desired to retain the static as well as dynamic mechanical, physical and electrical properties of MWCNT/PDMS composites. Uniform dispersion of nanofillers is of prime importance and contributes mainly to performance of the sensors [31].

Although these polymer nanocomposites have the challenges of non-linearity, hysteresis and temperature drifts, they are effective for large strains, simple and cost-effective to fabricate. These advantages make them a better choice of sensing elements for applications requiring complaint materials such as electronic skin, electronic textiles and other large deformation measurements. For this reason, the work presented here employs MWCNTs in PDMS matrix for piezoresistive sensor arrays. MWCNTs purchased from Sigma Aldrich have >95% carbon, with nanotubes having outer diameters of 6–9 nm, length  $5\mu\text{m}$  and  $\sim 2.5\text{g/mL}$  density at room temperature. In order to check the screen printability of the MWCNT/PDMS composite solution, three different solution samples, having 1%, 3% and 5% as weight ratios, were prepared. MWCNTs were first dispersed in chloroform by using mechanical stirrer and kept in ultrasonic bath at frequency 40 kHz for 30 minutes. After uniform dispersion of nanotubes in the chloroform, PDMS (Dow Corning Sylgard 184) was mixed with the solution followed by mechanical stirring for 10 minutes. Composite solution was kept again in ultrasonic bath at 40 kHz for 3 hours. Cross-linking agent was added in 10:1 into the composite and degassed completely in desiccator. Similar steps were followed for developing all the three solution samples [12]. After degassing steps, nanocomposites were immediately screen printed on pre-printed electrodes.

### C. Schematic of the Sensor Module

The scheme of each of the four sensor modules developed by using above synthesized materials is shown in Fig 1. Stencil mask has been developed in such a way that four modules (each with  $4 \times 4$  tactile sensors) can be printed on a single substrate in one go. A parallel plate structure is developed in which the transducer material is sandwiched between metallic layers. For metallic plates and interconnect lines as well, silver (Ag) based paste (purchased from DuPont (5028)) is used. Rheological properties of the Ag paste are already adjusted to be used with screen printing tools. UV-curable

dielectric (DuPont-5018) paste is used as received from supplier for the force concentrator structures. Details of the screen printing steps are discussed in the following sections.

## IV. SCREEN PRINTING EXPERIMENTS

### A. Screen Printing of Metallic Patterns and P(VDF-TrFE)

Different fabrication technologies have been reported to realize P(VDF-TrFE) based sensors. Spin coating, thermally drawn functional fibers, micro-machined mold transfer, single and multi-layer inkjet printers have been employed for developing P(VDF-TrFE) based sensors [6], [20], [21], [34]–[37]. The frequently used techniques such as spin coater and inkjet for patterning PVDF have limitations of process speed and overlay registration accuracy in multilayer structures. In addition, patterning of PVDF after spin coating whole layer on wafer requires photolithography, which leads to more complexity of the manufacturing process. Screen-printing is considered preferable alternative technology for patterning. For realizing the parallel plate capacitive structures the silver (Ag) based paste is used for top and bottom electrodes. Paste viscosity is in the range of 15-30 Pa.s. Conductive tracks for bottom electrodes are divided into 4 modules, each containing  $4 \times 4$  array of transducer components (Fig. 1). Capacitive area is  $1 \times 1\text{mm}^2$ , which are connected through printed interconnected lines of  $100\mu\text{m}$  wide. Distance between consecutive sensors is 5.6 mm in order to reduce crosstalk between neighboring sensors. The pads for readout signals,  $2 \times 2\text{mm}^2$  area, are coupled with printing bottom electrodes. After completing the first step of Ag printing, samples are sintered at  $120^\circ\text{C}$  for 1 hour. A separate stencil mask with  $3 \times 3\text{mm}^2$  opening area, overlapping on each side of the bottom electrode is used for printing piezoelectric material i.e. P(VDF-TrFE) on bottom electrode. Both stencil masks are designed in such a way that the overlay registration accuracy can closely be maintained. Screen-printing parameters i.e. squeegee height, pressure on the stencil, squeegee speed, snap-off and offset for the screen stage are critical to monitor. Height for first forward squeegee is kept at 46.15mm while the following squeegee is kept at 42.90 mm from the stencil mask. Pressure and speeds for both the squeegees are kept at 0.5 kg and 10 mm/sec respectively. Screen height from stage is kept at 5 mm while keeping the snap off at 1 mm. Deposited layers are sintered in vacuum at  $130^\circ\text{C}$  for 4 hours to remove the solvents and enhance recrystallization of P(VDF-TrFE). The top electrodes are patterned on separate PET substrate by using the first stencil mask but with  $90^\circ$  degree orientation to obtain sensors in the row-column fashion. The scheme of the stencil masks used for printing various sensor structures i.e. metallic patterns, transducer and dielectric for top force concentrator are shown in Fig 2(a).

Screen-printing is more robust and it is easy to control the layer thickness by varying process parameters like pressure and speed of the printing squeegee if solution properties have reached its optimal requirements. The small fraction of solution printed only at the opening of the stencil plays an important role in reducing material cost by minimizing wastage, and reusability of the solution makes the printing

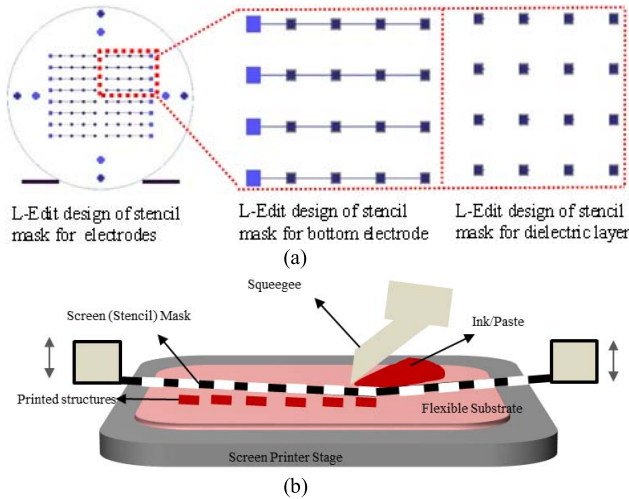


Fig. 2. (a) L-Edit design of stencil masks for metallic, transducer and force concentrator structures. (b) Schematic of flatbed screen-printing system setup.

TABLE I  
SCREEN PRINTING PARAMETERS

Material		Pressure(kg)	Snap-off (mm)	Speed (mm/sec)
PVDF-TrFE		0.5	1	10
MWCNT/PDMS	1%	0.45	1.2	15
	3%	0.5	1	10
	5%	0.5	1	6

system very robust for subsequent uses. However, the residual solution collected by the second squeegee is not completely the same as before and some part of the material is wasted in this process as well. This problem is mainly due to the selection of solvent specifically in case of P(VDF-TrFE) when dissolved in MEK. This problem is foreseen to overcome by investigating an appropriate solvent that is also compatible with screen-printing. Uniformity of the layer is maintained in screen-printing and the solution is deposited at desired areas of interest, i.e. on top of bottom metal layers with 100% overlay registration.

### B. Screen Printing of MWCNT/PDMS

The same structure of parallel plates and experimental setup is also followed to realize the piezoresistive sensors array. The MWCNT/PDMS nanocomposites layer is sandwiched between the two printed silver metal electrodes as discussed in previous section. Attractive feature of this approach is that the processing steps are performed by using a single printing technology i.e. screen-printing. Solutions of MWCNT/PDMS composites were printed on bottom electrode aligned by adjusting screen printing stage parameters. In case of MWCNT/PDMS the three solutions, with 1, 3 and 5% wt. prepared as reported in Sec. III B, were used for analysis of optimal dispensing out of the solution. Different printing speeds are applied because of different concentration of the three solutions. Speed of the forward squeegee was kept higher i.e. 15mm/sec in case of 1% solution and was decreased to 10 mm/sec and 6 mm/sec for 3% and 5% respectively. The experimental parameters such as squeegee pressure, snap-off from stage and speed are summarized in Table 1. High speed of the squeegee is observed

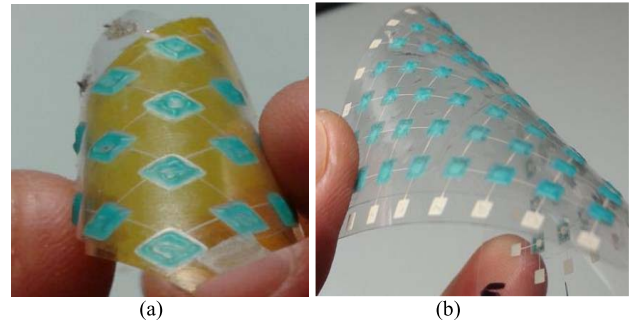


Fig. 3. Final assembled screen-printed sensor cells with force concentrated structures. (a) Sensors based on P(VDF-TrFE) on polyimide (PI) substrate. (b) Screen printed MWCNT/PDMS sensors on PET substrate.

to overcome the problem of bleed out of lower concentration solutions from the stencil mask, which also helps in keeping the desired patterns on the substrate after printing. This is the reason to keep the amount of dispensed material as minimum as possible. While at higher concentrations, speed is reduced to increase the dispense time at the stencil openings. These parameters were adjusted after doing a number of experiments with the prepared nanocomposite solutions. Deposited layers were sintered in vacuum at 80°C for 5 hours and kept overnight. After complete polymerization, counter electrode was printed on top of composite material using the same stencil but with 90° orientation. Top and bottom electrodes are in good alignment and no short-circuiting was found after checking all the devices. Force concentrator structures ( $3 \times 3 \text{ mm}^2$ ) were printed on a separate substrate and laminated on the bottom substrate, which also served as an encapsulant from any environmental affects to the sensors. Force concentrators were printed using UV-curable dielectric ink supplied by DuPont. Fig. 3(b) shows the final assembled array of sensor devices with force concentrator structures based on printing MWCNT/PDMS composites.

## V. RESULTS AND DISCUSSION

Screen-printed conductive patterns and sensitive materials were characterized to investigate different physical and electrical parameters required for reliable printed flexible sensor modules. In case of conductive patterns, the thickness of printed layers is of prime importance for enhanced electrical conductivity. Screen-printing deposits thick layers in a single deposition step as compared to other patterning tools by maintaining the overlay registration accuracy and uniform pattern edges, which is suitable for the proposed printed capacitive structures. Profilometer for thickness measurement, adhesion to the polymer substrate under different humidity and temperature conditions, print efficiency and sheet resistance are some of the prime characteristics of printed patterns. Adhesion of the subsequent printed materials on the sintered Ag patterns was checked in planar as well as in bent orientation of the substrate at 15mm radius. Finally, sensors are characterized by applying normal compressive forces at different frequencies. Results based on physical characteristics and responses with both materials are investigated and discussed in the following sub-sections.

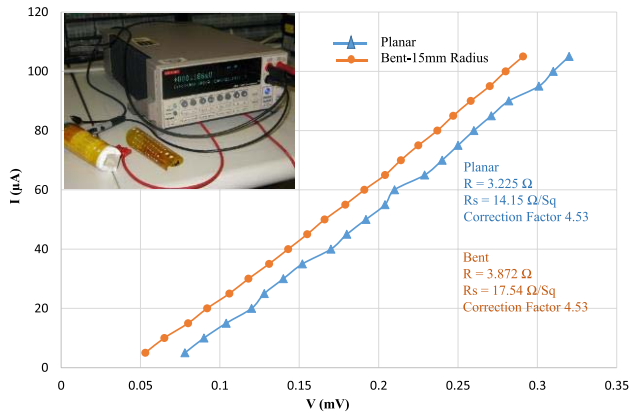


Fig. 4. Sheet resistance of screen-printed Silver (Ag) patterns in planar and bent orientation (radius 15 mm) on PI substrate.

#### A. Sheet Resistance of the Conductive Patterns in Planar and Bent Orientation

Sheet resistance of the conductive patterns has been measured in planar and bent mode to check any change in conductivity. Four-point collinear probe setup was developed by using high impedance Keithly 7410 voltmeter for current and voltage analysis (equipment shown in Fig.4). Resistance is measured in one complete row of printed electrodes having four plates connected inline. In the collinear configuration, the outer two probes placed at the centers of printed plates were used to source the current while the inner two probes placed on the central two plates were used to determine the voltage drop across the whole line. The sheet resistance value given by the supplier for the printed silver paste is about  $12\Omega/\text{sq}$ , for the layer with thickness about  $25\mu\text{m}$ . The sheet resistance measured in our samples (layer thickness of about  $8\mu\text{m}$ ) is  $14.15\Omega/\text{sq}$  in the planar mode, which is in the close range of expected sheet resistance of silver paste after sintering. The sheet resistances of the same printed lines were checked at bent orientation of the substrate. In bent orientation with radius of 15mm round, the sheet resistance was observed to be little higher i.e. about  $17.54\Omega/\text{sq}$ . This could be due to the variation in layer thickness and possible microcracks during the bend mode conditions. Nonetheless, the resistances in both the planar and bent orientations are acceptable for our application in the pressure sensors.

#### B. Microscopic and Mechanical Profilometer Analysis

Mechanical profilometer and scanning electron microscope (SEM) were used to analyze the thickness of conductive patterns as well as the deposited P(VDF-TrFE) and MWCNT/PDMS layers. Samples were analyzed after complete sintering in a vacuum environment. Fig 5 shows SEM image of P(VDF-TrFE) layer deposited on top electrode respectively. The porous structure observed in P(VDF-TrFE) layer indicates complete evaporation of solvent leaving behind pinholes. The printed layer of P(VDF-TrFE) in which the pinholes left after evaporation of the solution are evident from Fig 5. The Ag paste printed for top electrodes pass through these pinholes of the P(VDF-TrFE) layer, which eventually results in short circuiting of the two printed

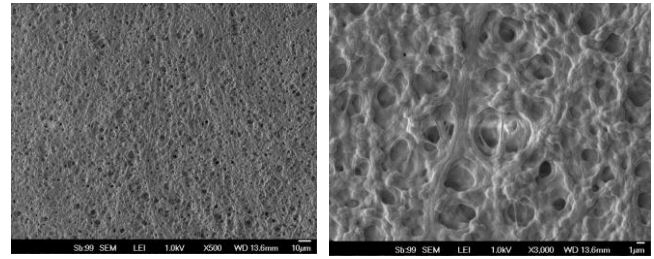


Fig. 5. Scanning electron microscope images showing optical micrographs of porous structure of screen-printed P(VDF-TrFE) on top of Ag patterns.

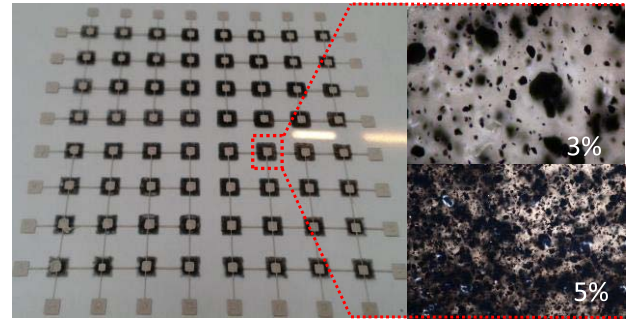


Fig. 6. Optical micrographs of screen-printed Ag (for metal and interconnect lines) and sandwiched MWCNT/PDMS. Optical microscopic images of 3 and 5% wt. shows the MWCNTs distribution in the PDMS matrix.

metal plates. This was confirmed by a trial experiment by printing Ag paste on top of P(VDF-TrFE), which resulted in short circuiting after sintering. This is one of the reasons for printing top electrode on a separate PET substrate instead directly on P(VDF-TrFE) due to the penetration of Ag paste through these pinholes.

Mechanical profilometer is used to check the thickness of all layers i.e. conductive patterns, P(VDF-TrFE) and MWCNT/PDMS layers. Metallic patterns observed at different positions of the substrate were found to have thickness about  $8\mu\text{m}$ . Screen printed P(VDF-TrFE) was found to have thickness about  $3\mu\text{m}$  less than the MWCNT/PDMS samples which were around  $10-15\mu\text{m}$  thick. Minimum thickness was obtained with the 1% solution, while layer with 5% solution is about  $15\mu\text{m}$ , which is due to the increased concentration of MWCNTs. Fig.6 shows the optical micrographs of the printed MWCNT layers in which agglomeration of MWCNT in the PDMS matrix occurs at random locations. Agglomeration of MWCNTs are more evident in solutions with increased concentrations of the filler materials that ultimately affects the reliability of the sensor response and consistency.

#### C. Adhesion Loss Test of Printed Layers at Different Humidity Level and Temperatures

It is important to determine the adhesion of printed features on polymeric substrate under different environmental conditions, especially the temperature and humidity as they have direct bearing on the reliability of sensors. Adhesion of screen-printed P(VDF-TrFE), MWCNT/PDMS, silver patterns and dielectric ink (for force concentrator structures) were checked under different temperature and humidity conditions. Tape test was performed for checking adhesion loss or complete delamination of the printed layers from flexible substrate.

TABLE II  
ADHESION LOSS TEST FOR THE PRINTED STRUCTURES

Printed Layer	Temp, °C	Absolute humidity, g/cm <sup>3</sup>	Observation delamination
Interconnect Lines	25	16	Negative
	40	40	Two lines (12% of the total length) delaminated.
	80	80	Three Lines (18% of the total length) delaminated.
Dielectric (Force Concentrators)	25	16	Negative
	40	40	Negative
	80	80	Negative
P(VDF-TrFE)	25	16	Negative
	40	40	Complete delamination
	80	80	Complete delamination
MWCNT/PDMS	25	16	Negative
	40	40	Negative
	80	80	Negative

Adhesion of these layers was investigated under two orientation schemes, first with samples on a planar surface and second, with substrates wrapped around a cylinder of 15 mm radius. Three different temperature and humidity conditions were developed for both the schemes as given in Table II. In first set of experiments, samples were tested at room temperature and humidity of 16g/cm<sup>3</sup>. In the second set of experiments, samples were placed in a humidity chamber with absolute humidity at 40 g/cm<sup>3</sup> and temperature at 40°C. The samples were kept in humidity chamber for 15 minutes and then taken out for adhesion test immediately. In the third setup, the humidity level was raised to 80 g/m<sup>3</sup> and temperature to 80 °C. Adhesion tape was applied on the samples immediately after withdrawal from the chamber for second and third set of experiments. At room temperature and 16 g/cm<sup>3</sup> of humidity, no delamination of interconnect wires or force concentrator structures were observed. Only two interconnect lines at the centers (12% of the total interconnects length) were peeled off at 40°C and absolute humidity of 40 g/cm<sup>3</sup>. For 80°C and 80g/cm<sup>3</sup> of the temperature and humidity, three interconnect lines of (18% of the total interconnects) were observed to be delaminated.

Similar results of delamination of interconnect lines were observed in bent orientation at 15 mm of radius, at the same conditions of humidity and temperature. Force concentrator structures were observed to have very good adhesion to the substrate and all the structures remained fixed. Adhesion loss test for printed structures of P(VDF-TrFE) was also performed according to the developed conditions mentioned above. Upon testing at room temperature, there is no peel-off of any structure from the substrate. However, at higher values of humidity and temperature in second and third set of experiments, all the layers of screen-printed P(VDF-TrFE) were peeled off. The same results were experienced for bent samples as well. The porous structures of P(VDF-TrFE) layer is playing critical role in absorbing the humidity, which ultimately weakens the materials/substrate interface strength and deteriorates all the structures developed

on top of it. The poor adhesion of P(VDF-TrFE) with polymer substrate at increased temperature and humidity values make it less attractive on an electronic skin, which is required to read stimulus accurately at varied working environment. Possible solution to the humidity problem is to use an encapsulation layer. The PET substrate used for top electrodes and force concentrator structures is selected to serve this purpose in our proposed scheme.

Plasma oxidation of polymer substrate was performed before printing bottom electrodes for modification of the surface to promote the adhesion of transducer materials with substrate. The plasma oxidation makes the polymer surface hydrophilic and improves the adhesion. As the total coverage area of the transducer material (3 × 3 mm<sup>2</sup>) is greater than bottom electrode (1 × 1 mm<sup>2</sup>), materials make strong bond around the electrodes after sintering. Polymer nanocomposites i.e. MWCNT/PDMS are soft material owing to the intrinsic properties of base polymer matrix. When microstructures of these composites are printed onto the plasma-oxidized substrate, the interface is tightly secured by strong bonding. Tape test was performed for checking adhesion loss of Ag tracks printed on top of MWCNT/PDMS nanocomposite. Adhesion of Ag is also found to be dependent on filler concentration. For 1% MWCNT/PDMS, about 70% of the Ag tracks were delaminated by peeling-off the adhesive tape. Adhesion became stronger for MWCNT/PDMS samples with higher concentrations, (i.e. with 3% and 5% filler concentrations), as about 50% and 10% of the Ag layers were delaminated respectively. This might be due to strong interaction of Ag paste on molecular level with MWCNTs in the PDMS matrix. Alternate to P(VDF-TrFE), MWCNT/PDMS showed very good adhesive properties at all the developed conditions of temperature and humidity. Surface properties of substrates for both the materials were modified by exposing it to plasma oxidation before doing printing experiments due to which adhesion of MWCNT/PDMS improved further, while no improvement in P(VDF-TrFE) was observed.

#### D. Capacitance-Voltage (C-V) and Piezoelectric Response of P(VDF-TrFE)

Polarization or poling of P(VDF-TrFE) is required to introduce the piezoelectric behavior. P(VDF-TrFE) is normally polarized by applying high voltage across the film. The strength of this voltage is typically 80 V/μm for P(VDF-TrFE) films [20]. This is one extra (and major) step towards achieving precise piezoelectric response. Higher voltage and increased charge induction to thin layers at raised temperatures often results in sparking and eventually destroy the structures. On the other hand, no modification or changes into the printed layers of MWCNT/PDMS are needed. The transduction paths developed by MWCNTs in PDMS bulk remain fixed after polymerization, which ultimately contribute to the change in resistivity. To polarize screen-printed P(VDF-TrFE), the sensor arrays were put on a hot plate at 80°C and voltage increased at a rate of 60 V/μm across the metal layers on the pads. For screen-printed layers of P(VDF-TrFE) with thickness of 3 μm, the maximum potential

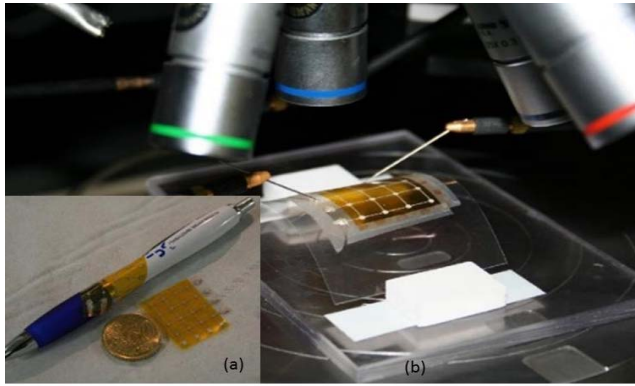


Fig. 7. (a) Final assembled sensor modules in planar and bent orientations. (b) C-V measurement setup of sensors in bent orientation.

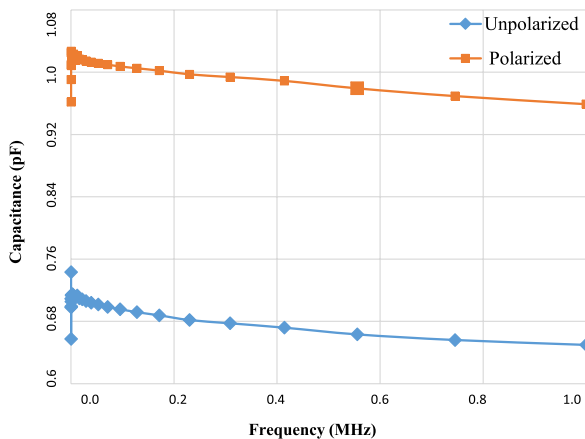


Fig. 8. Capacitance vs. frequency measurement of unpolarized and polarized P(VDF-TrFE) with peak oscillating voltage 10 mV and a hold time of 1s.

of 180V was reached in 6 incremental steps of 30V each. Electric field was applied for 10 minutes at each incremental step. Between two successive voltage application steps, the metal plates of P(VDF-TrFE) samples were short-circuited for about 5 minutes to mitigate the electric breakdown.

C-V measurements at varying frequencies were made before and after polarization. For C-V measurements, Agilent 4284A, precision LCR meter was used controlled by a program developed in LabVIEW. Fig. 7 shows arrangement of probes with sensor module in bent mode. The frequency used for experiment was increased in 30 steps ranging between 100Hz and 1MHz and peak oscillating voltage was kept at 10mV and hold time of 1 sec.

Average values of capacitance at all these frequencies before and after polarization are obtained and are 0.695 pF and 0.962 pF for unpoled and polarized samples respectively shown in Fig. 8. Change in capacitance value is observed in the polarized samples and an increase in capacitance of 0.267 pF is recorded. This difference is consistent among various capacitive devices both polarized and nonpolarized. This change may be due to polarized charges injected during poling. The general frequency response of the device is in the acceptable ranges as discussed in literature for applications to flexible pressure sensors.

Piezoelectric properties of the discrete devices were investigated at different frequencies and force values. Sensors were

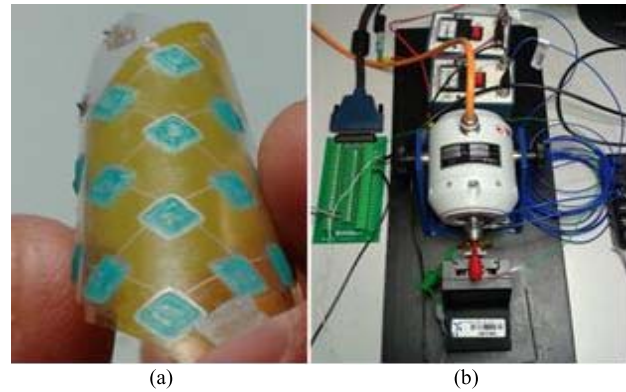


Fig. 9. Experimental setup of measuring piezoelectric response of P(VDF-TrFE). (a) Sensor module with force concentrator structures. (b) TIRA shaker and signal conditioning setup for dynamic force measurement.

tested at 10Hz, 50Hz and 200Hz while forces varied from 0.5–3.0 N for each corresponding frequency. Equipment used for testing the sensor devices consist of TIRA shaker, signal conditioning circuits and an amplifier shown in Fig. 9. All the major equipment for analysis and measurement of the output values is controlled by a program developed in LabVIEW. Upper limit of the dynamic force applied by shaker is 18 N with frequency ranging from 2 Hz–1 kHz. A load cell (PCB piezotronics) with sensitivity of 112.41mV/kN and measurement range of 0.00448 kN is mounted on the shaker tip, which can move in z-direction is used to measure and control the applied force on the sensor.

The force concentrators covering the whole effective area of the sensor is aligned according to the load cell tip in x, y and z directions. Sensors were characterized at constant frequency and increasing the applied force. At frequencies below 50 Hz, sensor response is about  $\sim 0.05\text{V/N}$ . For frequencies greater than 100Hz the response of the sensor increases approximately in linear fashion. This increase in response can be observed in Fig. 10 at 3N, which shows an increase of almost 0.07V for 200Hz and 0.02V for 100Hz at the same applied force. Response of the individual sensors at different value of frequencies and varying force is given in Fig. 10.

#### E. Piezoresistance Response of Printed MWCNT/PDMS Composite Sensors

The piezoresistance in MWCNT/PDMS nanocomposites is introduced by generation of distributed conductive paths within the bulk. The resistance of the sensors presented here can be tuned with filler concentration as shown Fig 11. This change in the initial resistance values for bulk piezoresistive composites at different filler concentration is mainly due to different number of interconnection paths and random distribution of MWCNT within the polymer matrix. Filler concentration is not only the major parameter for resistance change but is also critical for printing process. Solution becomes dense with increased amount of fillers and beyond a certain limit; it becomes difficult to screen print uniformly. Thus, an optimum range of filler concentration is required for controlled patterning and readable resistive response. At low

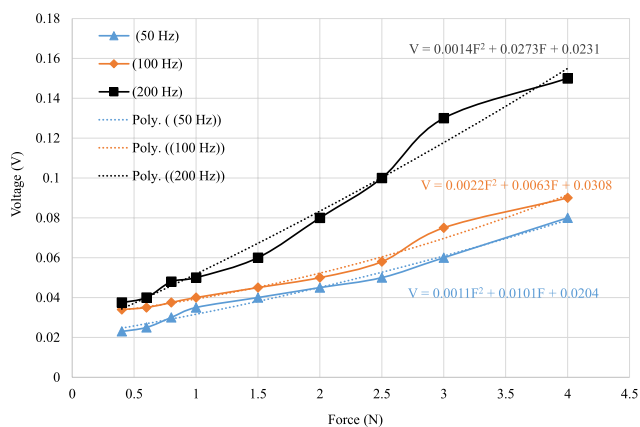


Fig. 10. Response of P(VDF-TrFE) at varying forces and frequencies. Sensor is characterized at three different frequencies i.e. 50, 100 and 200 Hz at each force value. Response of the sensor increases with increasing frequency while trend of graph lines is polynomial of second degree.

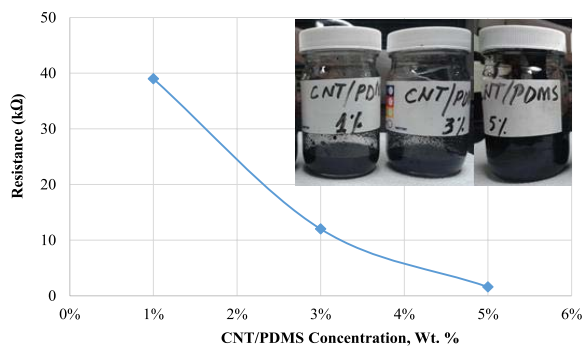


Fig. 11. Change in the resistance of polymerized composite samples with varying MWCNT concentration in PDMS.

concentrations  $\sim 1\%$ , the initial resistance is very large restricting resistance change within close limits. In addition, the solution is less viscous and flows out after printing which deteriorates the shape of the patterned structures. The isolation of individual sensing devices is not maintained and very irregular layer of MWCNT/PDMS is achieved. Avoiding such condition requires increase in the filler concentration. This also improves both physical and electrical properties of the device. With increased concentration, operating range of the device is extended due to an increase in the offset value of initial resistance. The operating envelope (0-10N for MWCNT/PDMS in current research) of the transducer material becomes responsive to an increased range of forces. Comparing the three nanocomposite solutions, 3% wt is found to be the optimum concentration by analyzing the piezoresistance response values in Fig 12 and also from screenprinting experiments.

The response of MWCNT/PDMS composites is obtained by applying compressive forces on the sensor device. The observed change in the resistance of sensors is due to (a) micro-nanoscale changes in the carbon nanotubes as a result of mechanical deformation, and (b) the formation of conductive paths within the matrix. Prepared samples were put on a rigid surface and force was applied on top of force concentrator structures that are aligned with the sensory cells. Piezoresistive behavior was confirmed by the observed change in resistance with respect to applied force. As shown in Fig 12,

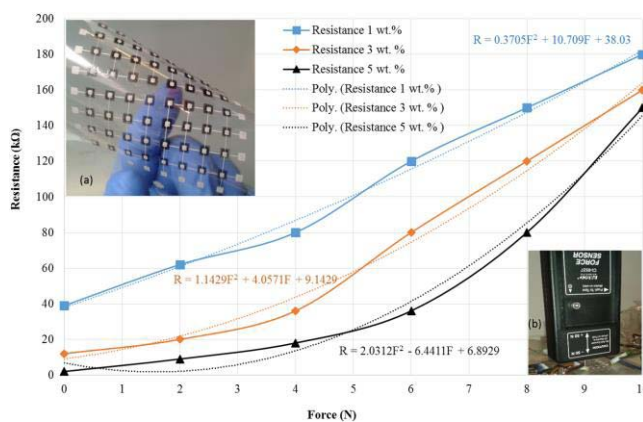


Fig. 12. Resistance change with normal compressive force showing trend line of a polynomial of degree two, (a). Screen-printed (MWCNT/PDMS 3% wt.) modules. (b) Setup of force sensors for characterizing final assembled device with force concentrator structures.

the resistance increases with increasing forces. The amount of change in the resistance values is observed to be higher for sample with less concentration of MWCNTs in PDMS. That could be due to immediate breakdown of the conduction paths established in the polymer matrix. The MWCNT/PDMS samples with 1% and 3% wt concentrations show an approximate linear response (Fig 12) which is often desired in pressure sensors. In case of 5% wt an abrupt non-uniform change in resistance occurs above forces of around 6N. This range is much higher than the force (0.01-1N) experienced by humans in daily tasks [14].

The sensors were also evaluated for cyclic force to check their restoration behavior to the initial resistances. Restoration of the resistance values for 3% wt after removing the applied stress was much faster than the samples with 1% and 5% wt concentrations. For 3% wt, the restoration time is of the order of few seconds, while for other two concentrations it took few minutes to restore the initial value. The trend of increase in resistance values is not uniform, which might be due to nonuniform dispersion and random conductive paths made by aggregates of nanotubes within the polymer matrix. Agglomeration of MWCNTs at various locations of the layers was observed after printing as shown in the optical micrographs in Fig 6. The agglomeration of MWCNTs occurred only in 3% and 5% wt. solutions. Agglomeration of nanotubes is more evident in less concentrated solution as compared to higher concentrations. Fluctuation in resistance values in bulk sample was observed at normal conditions without applying any stress or strain, which is possible due to the fast shifting of different conductive paths generated in the bulk MWCNT/PDMS composite (especially in higher concentrations and agglomerated sites). These fluctuations in resistance were observed even under compressive force on the devices.

Increase in resistance for all the three concentrations is detected when the substrates are wrapped in convex shape around a cylinder (15mm radius). This increase is caused by the bending induced strain. The conductive paths established during the normal position are enlarged which results in an increased resistance. Alternatively, decrease in resistance is recorded when the substrates are bent in concave shape.

In this case, the conductive paths are pushed more closer, which results in increase in conductivity of the composite. This is interesting for robotic skin when mounted especially at joints, where contraction and relaxation during the movement can be monitored and controlled by using such type of strain sensors.

## VI. CONCLUSION AND FUTURE WORK

Arrays of all screen printed flexible pressure sensors presented here were obtained by sandwiching P(VDF-TrFE) and MWCNT/PDMS separately between two patterned silver layers. A total of 64 sensors have been fabricated in one flow by screen printing technique. Screen-printing is attractive for printed multilayered electronic devices by using materials, which do not have any compatibility issues if printed layer by layer. Investigative study based on ease of processing, robustness, time saving, material efficiency and compatibility of layer-by-layer structures has been performed. Based on the physical characteristics of the printed layers, MWCNT/PDMS (3% wt) nanocomposite show uniform patterned deposition and reusability of the solution for subsequent use. Based on the screen-printing experiments 3 wt. percentage solution of MWCNT/PDMS was observed to be close to the viscosity ranges required for screen-printing. In addition, the agglomeration in 3% wt is less as compared to higher concentrations, which leads to approximately linear response and less fluctuations in resistance values of the sensors. There is no issue of porosity in MWCNT/PDMS layer as observed in P(VDF-TrFE) which help in reducing the extra processing process steps required for top electrode on a separate substrate. Also contact resistance in P(VDF-TrFE) with top electrode is expected to be higher as both the layers are not in intimate contact which is assumed to be one of the major drawbacks of P(VDF-TrFE) layers. Adhesion loss tests performed at different humidity conditions show delamination of P(VDF-TrFE) layer and poor adhesion to plastic substrates at raised temperatures as opposed to MWCNT/PDMS layers. Encapsulant in the form of PET substrate having top electrode and force concentrator structures are used for covering P(VDF-TrFE) in order to avoid such conditions.

Maximum sensors response at optimum operating values for P(VDF-TrFE) and MWCNT/PDMS are 0.05 V/N and 20 k $\Omega$ /N respectively, which shows piezoresistive material to have broad range of response at static forces. The response of P(VDF-TrFE) devices is almost near to ideal linear response required for tactile sensing. An additional step of polarization is required to induce charges in P(VDF-TrFE) layer, which will enhance the sensor response. Albeit poor physical characteristics of screen printed layers, P(VDF-TrFE) is ideal for dynamic forces at wide range of frequencies, which is useful in slip detection for tactile sensors on robotic skin. Although conductive polymer composites have the disadvantages of non-linearity, hysteresis and temperature drifts, they are simple, cost-effective to fabricate and effective for large strains.

Future work will involve finding threshold for optimum concentration, enhancing dispersion and reducing agglomeration of MWCNT. The pressure-mapping device could be enabled for local differences of pressure by utilizing the patterning

capability of composite materials. Further investigation of compatible solvents for P(VDF-TrFE), which have low evaporation rate during the printing process and matching-well with the viscosity requirements of the system will be explored. Characterizing whole array of devices and analysis of interference or cross talk will be investigated in future work. Whole package of screen printed foldable pressure sensor is targeted for development of low cost electronic skin applications. Successful patterning of P(VDF-TrFE) and MWCNT/PDMS nanocomposites in single step with reduced uniform thickness and the piezo-responses obtained, show that these sensors could find an attractive field of applications in not only electronic skin but in almost every enabling technology of large area electronic transducer system which needs light weight sensing devices attached conformably onto the surface.

## REFERENCES

- [1] A. Nathan *et al.*, "Flexible electronics: The next ubiquitous platform," *Proc. IEEE*, vol. 100, no. 13, pp. 1486–1517, May 2012.
- [2] R. F. Pease and S. Y. Chou, "Lithography and other patterning techniques for future electronics," *Proc. IEEE*, vol. 96, no. 2, pp. 248–270, Feb. 2008.
- [3] R. S. Dahiya, P. Mittendorfer, M. Valle, G. Cheng, and V. Lumelsky, "Directions toward effective utilization of tactile skin: A review," *IEEE Sensors J.*, vol. 13, no. 11, pp. 4121–4138, Nov. 2013.
- [4] R. S. Dahiya and M. Valle, *Robotic Tactile Sensing—Technologies and System*. Dordrecht, The Netherlands: Springer-Verlag, 2013.
- [5] R. S. Dahiya, A. Adami, C. Collini, and L. Lorenzelli, "POSFET tactile sensing arrays using CMOS technology," *Sens. Actuators A, Phys.*, vol. 202, pp. 226–232, Nov. 2013.
- [6] H.-K. Lee, J. Chung, S.-I. Chang, and E. Yoon, "Real-time measurement of the three-axis contact force distribution using a flexible capacitive polymer tactile sensor," *J. Micromech. Microeng.*, vol. 21, no. 3, p. 035010, 2011.
- [7] R. S. Dahiya, A. Adami, L. Pinna, C. Collini, M. Valle, and L. Lorenzelli, "Tactile sensing chips with POSFET array and integrated interface electronics," *IEEE Sensors J.*, vol. 14, no. 10, pp. 3448–3457, Oct. 2014.
- [8] R. S. Johansson and J. R. Flanagan, "Coding and use of tactile signals from the fingertips in object manipulation tasks," *Nature Rev. Neurosci.*, vol. 10, no. 5, pp. 345–359, May 2009.
- [9] M. Dietze and M. Es-Souni, "Structural and functional properties of screen-printed PZT-PVDF-TrFE composites," *Sens. Actuators A, Phys.*, vol. 143, no. 2, pp. 329–334, May 2007.
- [10] K. Arshak, D. Morris, A. Arshak, O. Korostynska, and K. Kaneswaran, "Investigation into the pressure sensing properties of PVDF and PVB thick film capacitors," in *Proc. 29th Int. Spring Seminar Electron. Technol.*, May 2006, pp. 334–339.
- [11] S. Khan, L. Lorenzelli, and R. S. Dahiya, "Screen printed flexible pressure sensors skin," in *Proc. 25th Annu. SEMI Adv. Semicond. Manuf. Conf. (ASMC)*, New York, NY, USA, May 2014, pp. 219–224.
- [12] S. Khan, L. Lorenzelli, and R. S. Dahiya, "Bendable piezoresistive sensors by screen printing MWCNT/PDMS composites on flexible substrates," in *Proc. 10th Conf. Ph.D. Res. Microelectron. Electron. (PRIME)*, Grenoble, France, Jun./Jul. 2014, pp. 1–4.
- [13] S. Khan, S. Tinku, L. Lorenzelli, and R. S. Dahiya, "Conformable tactile sensing using screen printed P(VDF-TrFE) and MWCNT-PDMS composites," in *Proc. 13th IEEE Conf. Sensors*, Valencia, Spain, Nov. 2014, pp. 1–4.
- [14] R. S. Dahiya, G. Metta, M. Valle, and G. Sandini, "Tactile sensing—From humans to humanoids," *IEEE Trans. Robot.*, vol. 26, no. 1, pp. 1–20, Feb. 2010.
- [15] J. S. Dodds, F. N. Meyers, and K. J. Loh, "Piezoelectric characterization of PVDF-TrFE thin films enhanced with ZnO nanoparticles," *IEEE Sensors J.*, vol. 12, no. 6, pp. 1889–1890, Jun. 2012.
- [16] Y. Jia, X. Chen, Q. Ni, L. Li, and C. Ju, "Dependence of the impact response of polyvinylidene fluoride sensors on their supporting materials' elasticity," *Sensors*, vol. 13, no. 7, pp. 8669–8678, Jul. 2013.
- [17] J. Cheng, O. Amft, and P. Lukowicz, "Active capacitive sensing: Exploring a new wearable sensing modality for activity recognition," presented at the 8th Int. Conf. Pervasive Comput., Helsinki, Finland, 2010.

- [18] L. Pinna, R. S. Dahiya, and M. Valle, "SPICE model for piezoelectric bender generators," in *Proc. 16th IEEE Int. Conf. Electron., Circuits, Syst., Yasmine Hammamet, Tunisia, Dec. 2009*, pp. 587–590.
- [19] C. M. Costa, L. C. Rodrigues, V. Sencadas, M. M. Silva, J. G. Rocha, and S. L. Mendez, "Effect of degree of porosity on the properties of poly(vinylidene fluoride–trifluoroethylene) for Li-ion battery separators," *J. Membrane Sci.*, vols. 407–408, pp. 193–201, Jul. 2012.
- [20] R. S. Dahiya, M. Valle, G. Metta, L. Lorenzelli, and S. Pedrotti, "Deposition, processing and characterization of P(VDF-TrFE) thin films for sensing applications," in *Proc. 9th IEEE Sensors Conf.*, Lecce, Italy, Oct. 2008, pp. 490–493.
- [21] X. He and K. Yao, "Crystallization mechanism and piezoelectric properties of solution-derived ferroelectric poly(vinylidene fluoride) thin films," *Appl. Phys. Lett.*, vol. 89, no. 11, pp. 112909-1–112909-3, Sep. 2006.
- [22] J. Engel, N. Chen, N. Chen, S. Pandya, and C. Liu, "Multi-walled carbon nanotube filled conductive elastomers: Materials and application to micro transducers," in *Proc. 19th IEEE MEMS Int. Conf.*, Jan. 2006, pp. 246–249.
- [23] R. S. Dahiya and S. Gennaro, "Bendable ultra-thin chips on flexible foils," *IEEE Sensors J.*, vol. 13, no. 10, pp. 4030–4037, Oct. 2013.
- [24] J. J. Neumann, D. W. Greve, and I. J. Oppenheim, "Comparison of piezoresistive and capacitive ultrasonic transducers," *Proc. SPIE, Smart Struct. Mater., Sensors Smart Struct. Technol. Civil, Mech., Aerosp. Syst.*, vol. 5391, no. 230, pp. 230–238, Jul. 2004.
- [25] M. Okuyama, "Miniature ultrasonic and tactile sensors for dexterous robot," *Trans. Elect. Electron. Mater.*, vol. 13, no. 5, pp. 215–220, Oct. 2012.
- [26] A. A. Mohammed, W. A. Moussa, and E. Lou, "High-performance piezoresistive MEMS strain sensor with low thermal sensitivity," *Sensors*, vol. 11, no. 2, pp. 1819–1846, 2011.
- [27] W.-P. Shih *et al.*, "Flexible temperature sensor array based on a graphite-polydimethylsiloxane composite," *Sensors*, vol. 10, no. 4, pp. 3597–3610, 2010.
- [28] C.-L. Wu, H.-C. Lin, J.-S. Hsu, M.-C. Yip, and W. Fang, "Static and dynamic mechanical properties of polydimethylsiloxane/carbon nanotube nanocomposites," *Thin Solid Films*, vol. 517, no. 17, pp. 4895–4901, Jul. 2009.
- [29] M. Lu, A. Bermak, and Y.-K. Lee, "Fabrication technology of piezoresistive conductive PDMS for micro fingerprint sensors," in *Proc. IEEE 20th Int. Conf. MEMS*, Jan. 2007, pp. 251–254.
- [30] C.-X. Liu and J.-W. Choi, "Strain-dependent resistance of PDMS and carbon nanotubes composite microstructures," *IEEE Trans. Nanotechnol.*, vol. 9, no. 5, pp. 590–595, Sep. 2010.
- [31] C.-X. Liu and J.-W. Choi, "Improved dispersion of carbon nanotubes in polymers at high concentrations," *Nanomaterials*, vol. 2, no. 4, pp. 329–347, Oct. 2012.
- [32] J. Hwang *et al.*, "Poly(3-hexylthiophene) wrapped carbon nanotube/poly(dimethylsiloxane) composites for use in finger-sensing piezoresistive pressure sensors," *Carbon*, vol. 49, no. 1, pp. 106–110, Jan. 2011.
- [33] K. Chu, D. Kim, Y. Sohn, S. Lee, C. Moon, and S. Park, "Electrical and thermal properties of carbon-nanotube composite for flexible electric heating-unit applications," *IEEE Electron Device Lett.*, vol. 34, no. 5, pp. 668–670, May 2013.
- [34] V. F. Cardoso, G. Minas, C. M. Costa, C. J. Tavares, and S. Lanceros-Mendez, "Micro and nanofilms of poly(vinylidene fluoride) with controlled thickness, morphology and electroactive crystalline phase for sensor and actuator applications," *Smart Matr. Struct.*, vol. 20, no. 8, p. 087002, 2011.
- [35] G. Lestoquoy, N. Chocat, Z. Wang, J. D. Joannopoulos, and Y. Fink, "Fabrication and characterization of thermally drawn fiber capacitors," *Appl. Phys. Lett.*, vol. 102, no. 15, pp. 152908-1–152908-5, 2013.
- [36] O. Pabst, J. Perelaer, E. Beckert, U. S. Schubert, R. Eberhard, and A. Tünnermann, "All inkjet-printed piezoelectric polymer actuators: Characterization and applications for micropumps in lab-on-a-chip systems," *Organic Electron.*, vol. 14, no. 12, pp. 3423–3429, Dec. 2013.
- [37] L. Tongxiang, S. Wenzhen, T. Monbo, W. Yanghua, and L. Hengde, "Surface tension and screen printing precision," *Chin. Sec. Bull.*, vol. 41, no. 22, pp. 1930–1935, 1996.
- [38] X. Z. Niu, S. L. Peng, L. Y. Liu, W. J. Wen, and P. Sheng, "Characterizing and patterning of PDMS-based conducting composites," *Adv. Mater.*, vol. 19, no. 18, pp. 2682–2686, Sep. 2007.
- [39] H. S. Nalwa, *Ferroelectric Polymers—Chemistry, Physics and Applications*. New York, NY, USA: Marcel Dekker, 1995.



**Saleem Khan** received the master's degree in electronic engineering from Jeju National University, Jeju, Korea, and the B.S. degree in engineering from the Ghulam Ishaq Khan Institute of Engineering Sciences and Technology, Topi, Pakistan. During his master's course, his research interests were in the development of flexible thin-film electronics on plastic substrates employing electrohydrodynamic inkjet printing. He is currently pursuing the Ph.D. degree at the University of Trento, Trento, Italy, and his research is based within the Microsystems Technology Research Unit, Fondazione Bruno Kessler, Trento, under the supervision of Dr. R. Dahiya and Dr. L. Lorenzelli. His research focus is the development of printing routes for flexible electronics manufacturing using transfer printing of Si micro/nanostructures on plastic substrates.



**Sajina Tinku** received the combined master's degree in micro and nanotechnologies for integrated systems from the Politecnico di Torino, Turin, Italy, the Grenoble Institute of Technology, Grenoble, France, and EPFL, Lausanne, Switzerland, and the B.Tech. degree in applied electronics and instrumentation from the University of Calicut, Calicut, India. During her master's course, her research interests were in the design and optimization of the photo resist mask for the confinement of biomaterials in the preparation of DNA microarrays. She is currently pursuing the Ph.D. degree at the University of Trento, Trento, Italy, and the Microsystems Technology Research Unit, Fondazione Bruno Kessler, Trento, under the supervision of Dr. L. Lorenzelli and Dr. R. Dahiya. Her research focus is in the design and fabrication of functional contact lens for human health monitoring.



**Leandro Lorenzelli** received the Laurea degree in electronic engineering from the University of Genoa, Genoa, Italy, in 1994, and the Ph.D. degree in electronics materials and technologies from the University of Trento, Trento, Italy, in 1998. During the Ph.D. course, his research activity concerned the development of electrochemical CMOS-based microsensors. In 1998, he joined the staff of the ITC-irst Microsystems Division, Trento, and was involved in the realization of microsystems for biomedical, environmental, and agro-food applications. Since 2005, he has been responsible for the Microsystems Technology Research Unit, Fondazione Bruno Kessler, Trento. His main scientific interests are in the processing technologies for both biomicroelectromechanical system and microtransducers.



**Ravinder S. Dahiya** (S'05–M'09–SM'12) is currently a Senior Lecturer in Electronics and Nanoscale Engineering with the University of Glasgow, Glasgow, U.K. He received the Ph.D. degree from the Italian Institute of Technology, Genoa, Italy. He was with the Netaji Subhas Institute of Technology, New Delhi, India, the Italian Institute of Technology, Fondazione Bruno Kessler, Trento, Italy, and the University of Cambridge, Cambridge, U.K.

His research interests include flexible and printable electronics, tactile sensing, electronic skin, and robotics. He has authored over 90 papers, one book, and holds one patent. He received the Marie Curie Fellowship and holds the EPSRC Fellowship. He has worked on many international projects and currently coordinating the European Commission funded Initial Training Network on Electronic Skin.

Dr. Dahiya is on the Editorial Boards of the *IEEE SENSORS JOURNAL* and the *IEEE TRANSACTIONS ON ROBOTICS*. He was a Guest Editor of two Special Journal Issues. He represents the Robotics and Automation Society of the IEEE and is AdCom of the IEEE Sensor Council. He was a recipient of the University Gold Medal in 1999. He also received the best paper awards on two occasions at IEEE conferences.